Symbol Error Rate Analysis for M-QAM Modulated Physical-Layer Network Coding with Phase Errors

Yang Huang*, Qingyang Song*, Shiqiang Wang†, and Abbas Jamalipour‡
*School of Information Science and Engineering, Northeastern University, Shenyang 110819, P. R. China
†Department of Electrical and Electronic Engineering, Imperial College London, SW7 2AZ, United Kingdom
‡School of Electrical and Information Engineering, University of Sydney, NSW, 2006, Australia
Email: hyocean198927@gmail.com, songqingyang@ise.neu.edu.cn, shiqiang.wang11@imperial.ac.uk, a.jamalipour@ieee.org

***Abstract*—Recent theoretical studies of physical-layer network coding (PNC) show much interest on high-level modulation, such as M-ary quadrature amplitude modulation (M-QAM), and most related works are based on the assumption of phase synchrony. The possible presence of synchronization error and channel estimation error highlight the demand of analyzing the symbol error rate (SER) performance of PNC under different phase errors. Assuming synchronization and a general constellation mapping method, which maps the superposed signal into a set of M coded symbols, in this paper, we analytically derive the SER for M-QAM modulated PNC under different phase errors. We obtain an approximation of SER for general M-QAM modulations, as well as exact SER for quadrature phase-shift keying (QPSK), i.e. 4-QAM. Afterwards, theoretical results are verified by Monte Carlo simulations. The results in this paper can be used as benchmarks for designing practical systems supporting PNC.**

***Index Terms*—Communication systems; phase error; physical-layer network coding (PNC); symbol error rate (SER) analysis; wireless networks.**

I. Introduction

Physical-layer network coding (PNC) [1] is considered as a promising technology to improve the throughput performance of wireless relaying networks. It employs both the broadcast nature of wireless channels and the natural network coding ability introduced by the superposition of electromagnetic waves. Between the two methods of PNC, i.e. amplify-and-forward [2] and denoise-and-forward (DNF), the DNF method shows more performance advantages because it avoids noise amplification [3]. Hence, DNF has attracted much interest in recent research, and we also focus on DNF in this paper.

Recently, PNC (using the DNF method) with high-level modulations or nested lattice code attracts much interest [4]–[7], but these are generally based on the assumption of perfect synchronization. Although there is also some work focusing on asynchronous PNC [8]–[10], synchronous PNC still has advantages because it allows more efficient constellation design [4] and can make use of capacity-approaching channel codes [6]. The capacity region of the Gaussian two-way relay channel can also be reached with synchronous PNC [7].

Progress on phase synchronization has been achieved in both theoretical works [11], [12] and implementations [13], under the context of distributed beamforming, which is a similar superposition-based cooperative technology. A phase synchronization scheme for PNC was also recently proposed in [14]. However, the aforementioned synchronization schemes may suffer from untrackable phase errors [15]. Because the synchronization may not be perfect due to noise [16], the phase error between the signals keeps on increasing during the signal transmission period [11]. Also, in channels with imperfect channel state information (CSI), the phase error between signals may not be perfectly known to the relay [17]. The above problems affect the error performance of a practical system. Therefore, it is necessary to investigate how the phase error affects the performance of PNC, which we focus on in this paper.

In terms of error performance analysis for PNC, recent works focus on PNC with binary phase-shift keying (BPSK) or quadrature phase-shift keying (QPSK) [18]–[20]. The symbol error rate (SER) and bit error rate (BER) for BPSK and QPSK modulation was studied in [18] and [19], where a polar coordinates method proposed by [21] was exploited. Due to its complexity, the polar coordinates method is difficult to apply to high-level M-ary quadrature amplitude modulation (M-QAM) modulation. It is also not suitable for analysis with phase error, since the undesired phase rotation degrades the geometrical regularity and makes it difficult to associate the angle with the radius in polar coordinates. In [20], an approximation to the bit error rate (BER) for PNC with BPSK modulation over fading channels was obtained, but higher level modulations were not considered. Different from the existing works, we focus on the SER for M-QAM modulated PNC with arbitrary M and also consider different phase errors. The analysis with M-QAM is significant because M-QAM is widely applied to rate-adaptive communication systems.

In this paper, we analyze the SER for M-QAM modulated PNC with arbitrary phase error. We consider a general constellation mapping, which maps the superposed $(2\sqrt{M}-1)$ by $(2\sqrt{M}-1)$ constellation into a set of M coded symbols. By projecting the 2-dimensional signal onto the in-phase and quadrature axes, we derive an approximation of the SER for M-QAM analytically. Then we modify the results for general M-QAM and obtain the exact SER for QPSK, i.e. 4-QAM.

The remainder of this paper is organized as follows. Section II illustrates the system model and the decoding method, and discusses the ambiguity in constellation mapping. Section

Fig. 1. PNC over a bidirectional relay network.

III derives the approximation of the SER for M-QAM and the exact SER for QPSK under different phase errors. The analytical SER for M-QAM and QPSK is confirmed by the comparison with Monte Carlo simulations in Section IV. Conclusions are drawn in Section V.

II. Preliminaries

A. System Model

We consider a typical bidirectional relay network in which node R performs DNF relaying, as shown in Fig. 1. The DNF process includes multiple access (MA) phase and broadcast (BC) phase. In the MA phase, end nodes A and B transmit square M-QAM modulated data to the relay simultaneously. The signal Y_R received by R is given by

$$Y_R = S_A + S_B + Z_R\,, \tag{1}$$

where S_A and S_B denote M-QAM signals from A and B respectively, and Z_R is the additive white Gaussian noise (AWGN) at R. In this paper, perfect power control is assumed.

B. Minimum Distance Estimation

The minimum distance (MD) estimation is employed at the relay R to map the superposed signal Y_R to a network-coded symbol. With knowledge of CSI, the MD estimation can adjust decision boundaries. However, this feature may reduce Euclidean distances among adjacent constellation points when high-level modulation is performed. Although [9] proposed an adaptive mapping rule to address this problem, the end-to-end throughput may suffer huge penalty when error occurs in channel estimation [17]. Inspired by recent progress on phase synchronization [12], [14], in this paper, we consider PNC with phase-level synchronization, in which each constellation point (ideally) appears in the center of the corresponding decision region, which maximizes Euclidean distances.

Since a M-QAM signal can be viewed as a complex $\sqrt{M}$-ary pulse amplitude modulation ($\sqrt{M}$-PAM) signal, its in-phase component $I_R(k)$ and quadrature component $Q_R(n)$ can be extracted from the superposed constellation point $S_{k,n}$, i.e. $S_{k,n} = I_R(k)+Q_R(n)$. Euclidean norms of these components are given by

$$\|I_R(k)\| = 2(k-\sqrt{M})d\,, \tag{2}$$

$$\|Q_R(n)\| = 2(n-\sqrt{M})d\,, \tag{3}$$

where $k,n \in \{1,2,\cdots,2\sqrt{M}-1\}$, $\|\cdot\|$ stands for the Euclidean norm, and d denotes the Euclidean distance between two adjacent points in the constellation diagram for $\sqrt{M}$-PAM. Based on (2) and (3), there are $(2\sqrt{M}-1)^2$ different superposed constellation points ($S_{k,n}$). The MD estimation for $\hat{S}_{k,n}$ is given as

$$(\hat{k},\hat{n}) = \arg\min_{k,n} \|Y_R - (I_R(k)+Q_R(n))\|\,, \tag{4}$$

$$\hat{S}_{k,n} = I_R(\hat{k}) + Q_R(\hat{n})\,. \tag{5}$$

The estimated $\hat{S}_{k,n}$ will be mapped into a network-coded symbol.

C. Ambiguity in Denoise Mapping

The denoise mapping at the relay R is generally non-bijective when performing PNC, i.e. different superposed signals may be mapped into the same symbol. However, the well known XOR mapping method causes ambiguity that identical superposed signals are mapped into different symbols when high-level modulations are performed [4], [5]. The resolution proposed by [5] increases sum levels at R and adopts bijective mapping, which reduces Euclidean distances and excludes benefits from non-bijective mapping. Nevertheless, without increasing the number of constellation points, recent design to avoid ambiguity proposed by [22] maintains the non-bijective mapping.

For generality, in this paper, we assume a certain mapping rule $\mathcal{C}(\cdot)$ which is unknown but features both non-bijective mapping and unchanged number of constellation points, i.e. the $(2\sqrt{M}-1)^2$ superposed constellation points are mapped into M coded symbols. The network-coded symbol v is obtained by $v = \mathcal{C}(\hat{S}_{k,n})$. Subsequently, symbol v is transmitted in the BC phase and decoded by end nodes.

III. Error Performance Analysis

This section first analyzes the SER for M-QAM with arbitrary phase errors. Then, the specific case of QPSK (i.e. 4-QAM) is considered based on the results for general M-QAM.

A. Approximated SER for M-QAM Modulated PNC with Phase Errors

In this subsection, we derive an approximation of the SER for M-QAM modulated PNC with phase errors. It has been proven that the necessary and sufficient condition of unique decodability for PNC with M-QAM is that points in any $\sqrt{M}$ by $\sqrt{M}$ square in the constellation for superposed signals at the relay R are mapped into different symbols [22]. When M is large enough, the AWGN can hardly let the superposed signal go across several decision regions and reach a region that should be mapped to a coded symbol that is identical with the correct symbol. Thus, assuming a large M, we can safely neglect the probability that superposed signals appear in other identical-mapping regions. The numerical results in Section IV reveal that an M of 16 is adequate for this assumption to hold, while we can get an exact result when $M = 4$.

As depicted in Fig. 2, M-QAM signals S_A and S_B from A and B can be regarded as the combination of orthogonal $\sqrt{M}$-PAM signals. S_A is decomposed into mutually orthogonal components I_A and Q_A, and, likewise, S_B is divided into

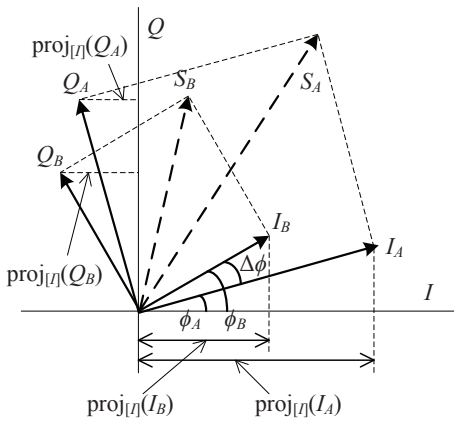

Fig. 2. Geometric representation of the received M-QAM signals S_A and S_B at the relay R in vector space. Signal vectors S_A and S_B rotate ϕ_A and ϕ_B from the reference, respectively.

I_B and Q_B. The Euclidean norms of these components are given as

$$\|I_A\| = (2i - 1 - \sqrt{M})d\,, \tag{6}$$
$$\|Q_A\| = (2i' - 1 - \sqrt{M})d\,, \tag{7}$$
$$\|I_B\| = (2j - 1 - \sqrt{M})d\,, \tag{8}$$
$$\|Q_B\| = (2j' - 1 - \sqrt{M})d\,, \tag{9}$$

where $i, i', j, j' \in \{1, 2, \cdots, \sqrt{M}\}$ are the indexes of the constellation points, and d is obtained by [16]:

$$d = \left(\frac{3E_b \log_2 \sqrt{M}}{M-1}\right)^{1/2}, \tag{10}$$

where E_b represents the average bit energy of the received signal at the relay R. As illustrated in Fig. 2, phase drift in the carrier of S_A (which is composed of I_A and Q_A) is expressed as a rotation by an angle of ϕ_A. Likewise, the rotation of S_B (which is composed of I_B and Q_B) is ϕ_B from the axes. Since a receiver usually performs channel estimation through preambles [15], we assume that the receiver can only track the phase rotation from knowledge of the preamble at the beginning of each data frame. Hence, the receiver is unaware of these undesired rotations in the subsequent symbols, and the decision boundaries remain unchanged.

When the MD estimation is performed, decision regions of the constellation at the relay R are bounded by straight lines parallel to coordinate axes under the condition of power control and synchronization. Consequently, the MD estimation in the 2-dimensional space can be separately performed on channels I and Q (I-axis and Q-axis). Decision boundaries for each constellation point $S_{k,n}$ in channels I and Q are given by $2(k - \sqrt{M} \pm 1/2)d$ and $2(n - \sqrt{M} \pm 1/2)d$, respectively. Fig. 3 shows the decision boundaries in the I-channel, and any supposed constellation point without phase error on the I-axis is given by

$$\mu_0 = 2(i + j - 1 - \sqrt{M})d\,. \tag{11}$$

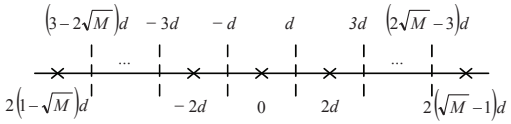

Fig. 3. I-channel decision boundaries for superposed M-QAM signals. The dashed lines denote decision boundaries and the crosses represent constellation points.

Assume the transmitted symbols are equiprobable, the error probabilities calculated on the I-axis and Q-axis are equal. Thus, we only focus on the decoding on the I-axis. As shown in Fig. 2, the superposed signal (with phase error) in the I-channel is given by

$$\begin{aligned}\mu = &\, proj_{[I]}(I_A) + proj_{[I]}(I_B) \\ &+ proj_{[I]}(Q_A) + proj_{[I]}(Q_B)\,,\end{aligned} \tag{12}$$

where $proj_{[x]}(y)$ denotes the orthogonal projection of the vector y into the line spanned by the vector x. Combining with (6)–(9), (12) can be rewritten as

$$\begin{aligned}\mu = &\, \|I_A\|\cos\phi_A + \|I_B\|\cos\phi_B \\ &- \|Q_A\|\sin\phi_A - \|Q_B\|\sin\phi_B\,.\end{aligned} \tag{13}$$

Considering the different intervals of decision regions as shown in Fig. 3, for given i, i', j and j', error probability is analyzed for different superposed constellation points (μ_0). In the case of $\mu_0 \neq 2(1 - \sqrt{M})d$ and $\mu_0 \neq 2(\sqrt{M} - 1)d$, i.e. $i + j \neq 2$ and $i + j \neq 2\sqrt{M}$, the error probability is obtained by

$$\begin{aligned}P_s(E)\Big|_{i+j\neq 2,2\sqrt{M}} &= \frac{1}{\sqrt{2\pi}\sigma}\int_{-\infty}^{\mu_0-d}\exp\left(-\frac{(x-\mu)^2}{2\sigma^2}\right)dx \\ &\quad + \frac{1}{\sqrt{2\pi}\sigma}\int_{\mu_0+d}^{\infty}\exp\left(-\frac{(x-\mu)^2}{2\sigma^2}\right)dx \\ &= Q\left(\frac{d+\mu-\mu_0}{\sigma}\right) + Q\left(\frac{d+\mu_0-\mu}{\sigma}\right),\end{aligned} \tag{14}$$

where $\sigma = \sqrt{N_0/2}$ denotes the standard deviation of AWGN in the I-channel and N_0 is the noise power spectral density. In the case of $\mu_0 = 2(1 - \sqrt{M})d$, i.e. $i, j = 1$, the error probability is given by

$$\begin{aligned}P_s(E)\Big|_{i,j=1} &= \frac{1}{\sqrt{2\pi}\sigma}\int_{\mu_0+d}^{\infty}\exp\left(-\frac{(x-\mu)^2}{2\sigma^2}\right)dx \\ &= Q\left(\frac{d+\mu_0-\mu}{\sigma}\right).\end{aligned} \tag{15}$$

When $\mu_0 = 2(\sqrt{M}-1)d$, i.e. $i, j = \sqrt{M}$, the error probability is achieved by

$$\begin{aligned}P_s(E)\Big|_{i,j=\sqrt{M}} &= \frac{1}{\sqrt{2\pi}\sigma}\int_{-\infty}^{\mu_0-d}\exp\left(-\frac{(x-\mu)^2}{2\sigma^2}\right)dx \\ &= Q\left(\frac{d+\mu-\mu_0}{\sigma}\right).\end{aligned} \tag{16}$$

For equiprobable symbols, any combination of (i, i', j, j') shares the same probability $1/M^2$. Combining (14), (15) and

(16), the error probability on the I-axis is given by

$$P_s(E)\Big|_{I\text{-axis}} = \frac{1}{M^2}\sum_{i',j'=1}^{\sqrt{M}}\left(P_s(E)\Big|_{i,j=1} + P_s(E)\Big|_{i,j=\sqrt{M}} + \sum_{i,j=1}^{\sqrt{M}} P_s(E)\Big|_{i+j\neq 2,2\sqrt{M}}\right). \quad (17)$$

Then, we can obtain the approximation to SER for M-QAM modulated PNC:

$$P_s(E)\Big|_{M\text{-QAM-PNC}} = 1 - \left(1 - P_s(E)\Big|_{I-\text{axis}}\right)^2. \quad (18)$$

B. Exact SER for QPSK Modulated PNC with Phase Errors

This subsection discusses the case of $M = 4$ (i.e. PNC is performed with QPSK) and analyzes the exact error probability under different phase errors. In Section III-A, we approximated the SER by neglecting the probability of identical mapping. It is well known that with XOR network coding, the constellation mapping for QPSK modulated PNC makes no ambiguity. Therefore, we can investigate an exact error probability for QPSK.

When PNC is performed with QPSK, the in-phase component is given by $I_R(k) \in \{-2d, 0, 2d\}$, and the mapping rule is that $\{-2d, 2d\}$ is mapped into bit "0" and $\{0\}$ is mapped into bit "1". Observing this "edge-identical" mapping, we modify (15) and (16), where μ_0 equals $2(1-\sqrt{M})d$ or $2(\sqrt{M}-1)d$, to achieve the exact SER for QPSK. Eqs. (15) and (16) can be combined as

$$P_s'(E)\Big|_{i,j=1 \text{ or } i,j=\sqrt{M}} = \frac{1}{\sqrt{2\pi}\sigma}\int_{-d}^{d}\exp\left(-\frac{(x-\mu)^2}{2\sigma^2}\right)dx = Q\left(\frac{\mu-d}{\sigma}\right) - Q\left(\frac{\mu+d}{\sigma}\right). \quad (19)$$

Let (19) be the substitutes for (15) and (16) in (17), and the exact SER for QPSK modulated PNC with phase error can be calculated with (18).

C. Constraint on Phase Errors

Phase errors or undesired phase rotations cause mitigation of desired signals and generate undesired projections such as the projection of Q_A and Q_B on the I-axis, as shown in Fig. 2. It is noted that the superposed signal μ may exceed decision boundaries and lead to erroneous decoding even without noise. Therefore, under any signal-to-noise ratio (SNR) value, μ should be restricted by $\mu \in (\mu_0 - d, \mu_0 + d)$ for any $i, i', j,$ and j'. According to (13), the values of phase errors are directly related to the value of μ. Hence, we can obtain a constraint of the relationship among ϕ_A, ϕ_B and M:

$$\cos\left(|\phi_A| + \frac{\pi}{4}\right) + \cos\left(|\phi_B| + \frac{\pi}{4}\right) > \frac{2\sqrt{M}-3}{\sqrt{2}(\sqrt{M}-1)}, \quad (20)$$

which can also be rewritten as

$$\rho(\phi_A, \phi_B) \triangleq \cos\frac{|\phi_A| - |\phi_B|}{2}\cos\left(\frac{|\phi_A| + |\phi_B|}{2} + \frac{\pi}{4}\right) > \frac{2\sqrt{M}-3}{2\sqrt{2}(\sqrt{M}-1)} \triangleq \beta(M), \quad (21)$$

where $\rho(\phi_A, \phi_B)$ and $\beta(M)$ are respectively defined as the metric for phase errors and the system bound to phase errors. The detailed derivation of (20) is shown in Appendix A.

To ensure that every point is in its own decision region, ϕ_A and ϕ_B must conform to (21). Since the cosine function is an even function and it decreases monotonically in the interval $[0, \pi]$, (21) reveals that the absolute values of the phase errors should be controlled to be approximately equal, and their totals should be restricted.

IV. Simulation Results

Considering different phase errors of ϕ_A and ϕ_B, this section confirms the analytical SER for M-QAM modulated PNC with Monte Carlo simulations. We perform simulations with 16-QAM and QPSK, to show the accuracy of the analytical approximation for general M-QAMs and the exact SER for QPSK. The constellation mapping method proposed in [22] is adopted for 16-QAM, and XOR mapping is used for QPSK. We investigate the theoretical and simulated values with different phase errors and under different SNR values.

Fig. 4 shows the comparison between simulated results and the analytical results for 16-QAM. It can be observed that although the approximation given by (18) neglects the probability of identical mapping, the simulated results nearly coincide with the analytical approximation. One reason is that when M is large enough, the regions that are mapped into identical coded symbols are far away. Thus, the gap between the approximated probability and the exact probability is small. It follows that the approximation to SER in (18) is effective and accurate for general M-QAMs.

Fig. 5 shows the comparison between the analytical exact SER for PNC with QPSK and its simulated results. It is apparent from Fig. 5 that the analytical results show good matches with the simulated results.

It is also observed in Fig. 4 that, when S_A and S_B suffer phase errors of $\phi_A = \phi_B = 8.8°$, the shape of the SER curve differs from the typical waterfall shape. The reason is that phase errors of $\phi_A = \phi_B = 8.8°$ make the value of $\rho(8.8°, 8.8°) = 0.5906$ approach the bound $\beta(16) = 0.5893$, according to (21). This means that, with phase errors of $\phi_A = \phi_B = 8.8°$, some constellation points nearly step on the decision boundaries, which may cause decoding errors even with high SNR.

For 16-QAM, when the phase errors are $\phi_A = \phi_B = 10°$, the constraint (21) is violated, because $\rho(10°, 10°) = 0.5736 < \beta(16)$. In this case, the SER does not keep decreasing with increasing SNR, but tends to converge to stable values, as shown in Fig. 4. The reason is that some superposed constellation points lie in erroneous decision regions even without noise, when (21) is not satisfied. Hence, (21) can be regarded as a condition for the SER curve to keep an asymptotically decreasing trend. A similar trend can be observed for QPSK with $\phi_A = \phi_B = 25°$, as shown in Fig. 5.

We also find in Figs. 4 and 5 that positive and negative phase errors can lead to the same SER, and it is only the

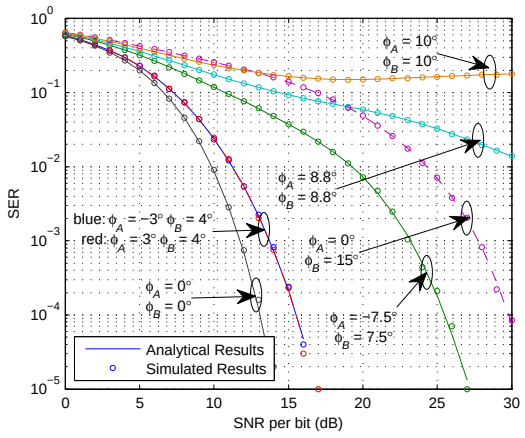

Fig. 4. SER for 16-QAM modulated PNC with the impact of phase errors.

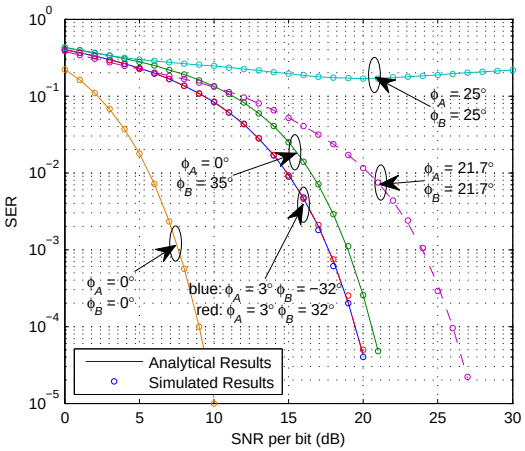

Fig. 5. SER for QPSK modulated PNC with the impact of phase errors.

absolute values of phase errors that matter. This is because the symmetry of the constellation makes the distances among constellation points and decision boundaries be identically distributed under positive and negative phase rotations, although the constellation shapes may be different. This observation is also in accord with the fact that only the absolute values of phase errors are used for calculation in (21).

Another interesting observation is that, in low SNR regions in Fig. 4, the SER curve for phase errors of $\phi_A = \phi_B = 8.8°$ outperforms the SER curve for phase errors of $\phi'_A = 0$ and $\phi'_B = 15°$. However, $\rho(0, 15°) = 0.6036 > \rho(8.8°, 8.8°)$, i.e. $\rho(0, 15°)$ is further away from $\beta(16)$. Similar phenomenon can also be observed for QPSK in Fig. 5, with the phase errors $\phi_A = \phi_B = 21.7°$ and $\phi'_A = 0$, $\phi'_B = 35°$. The reason is that the constraint (21) only corresponds to the worst case constellation points.

To investigate this phenomenon further, we take the superposed QPSK constellation as an example, as shown in Fig. 6. In the following discussion, we call case A for $\phi_A = \phi_B = 21.7°$ (Fig. 6(a)), and case B for $\phi'_A = 0$ and $\phi'_B = 35°$ (Fig. 6(b)). We can observe that, in case A, the constellation points that are mapped to symbols "00", "01", and "10" are close to decision boundaries, while the point that is mapped to symbol "11" still remains in the center of its original (when there is no phase error) decision region. In case B, the constellation points corresponding to "11" also move close to the boundaries. At low SNRs, it is very likely that those constellation points that are near to decision boundaries are mapped into erroneous symbols. The SER in case A is slightly lower than the SER in case B because, in case A, the symbol "11" can be correctly mapped with a higher probability. At high SNRs, the SER tends to be dominated by those constellation points that are closest to decision boundaries, because all the other points can be correctly mapped with a high probability when the SNR is high. Since $\rho(0, 35°) = 0.4404 > \rho(21.7°, 21.7°) = 0.3955 > \beta(4) = 0.3536$, the minimum distance between constellation points and boundaries is smaller in case A, compared with case B. Therefore, case A underperforms case B in high SNR regions. When we take a careful look at Fig. 6, we can find that the "00" points in case A are closest to the boundaries compared to any other point in both cases A and B.

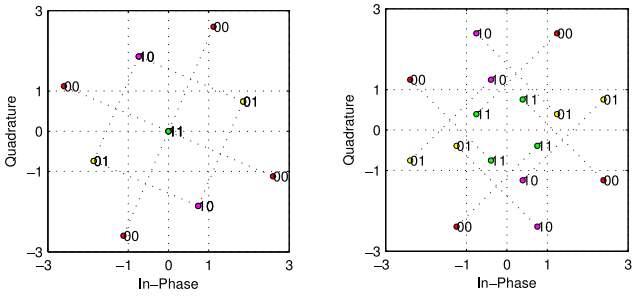

(a) $\phi_A = 21.7°$, $\phi_B = 21.7°$ (b) $\phi'_A = 0$, $\phi'_B = 35°$

Fig. 6. Constellation diagram for QPSK modulated PNC suffering different phase errors. Values of -1 and 1 on axes are the decision boundaries. For $M = 4$, system bound to phase errors is $\beta(4)$.

V. Conclusions

In this paper, we have analyzed the SER performance for PNC with M-QAM under arbitrary phase errors. In our analysis, we have considered a constellation mapping which maintains non-bijective mapping and the most common $(2\sqrt{M}-1)$ by $(2\sqrt{M}-1)$ constellation. For this mapping rule, we have obtained an accurate approximation to the SER for M-QAM and achieved the exact SER for QPSK, analytically. We have also obtained a constraint on the maximum acceptable phase error to keep the SER decreases with the SNR. Simulation results show agreement with the analytical results. The results in this paper can be used as benchmarks for the design of synchronization and rate-adaptation schemes in the future. We have been considering deterministic phase errors in this paper. The case with random phase errors and channel gains will be

considered in our future work.

APPENDIX A
DERIVATION OF CONSTRAINT ON PHASE ERRORS

To obtain the relationship among ϕ_A, ϕ_B and M, we substitute (6)–(9), (11) and (13) into $\mu \in (\mu_0 - d, \mu_0 + d)$. Let

$$\begin{aligned} f(\phi_A, \phi_B, M, i, i', j, j') &= (2i - 1 - \sqrt{M})d\cos\phi_A \\ &+(2j - 1 - \sqrt{M})d\cos\phi_B - (2i' - 1 - \sqrt{M})d\sin\phi_A \\ &-(2j' - 1 - \sqrt{M})d\sin\phi_B - 2(i + j - 1 - \sqrt{M})d, \end{aligned} \quad \text{(A.1)}$$

the constraint of ϕ_A and ϕ_B for given M can be expressed as

$$-d < f(\phi_A, \phi_B, M, i, i', j, j') < d. \quad \text{(A.2)}$$

Recall that $i, i', j, j' \in \{1, 2, \cdots, \sqrt{M}\}$. To make sure that (A.2) holds for any $i, i', j,$ and j', we need to have

$$\min_{i,i',j,j'} f > -d \text{ and } \max_{i,i',j,j'} f < d. \quad \text{(A.3)}$$

Also note that (A.1) can be rewritten as

$$\begin{aligned} f(\phi_A, \phi_B, M, i, i', j, j') &= (1 + \sqrt{M})(2 - \cos\phi_A - \cos\phi_B)d \\ &-(2i' - 1 - \sqrt{M})d\sin\phi_A - (2j' - 1 - \sqrt{M})d\sin\phi_B \\ &-2i(1 - \cos\phi_A)d - 2j(1 - \cos\phi_B)d. \end{aligned} \quad \text{(A.4)}$$

From (A.4), we can easily have

$$\arg\min_{i,j} f = (\sqrt{M}, \sqrt{M}), \quad \text{(A.5)}$$

$$\arg\max_{i,j} f = (1, 1), \quad \text{(A.6)}$$

$$\arg\min_{i',j'} f = \begin{cases} (\sqrt{M}, \sqrt{M}) & \text{if } \phi_A \geq 0, \phi_B \geq 0 \\ (1, \sqrt{M}) & \text{if } \phi_A < 0, \phi_B \geq 0 \\ (\sqrt{M}, 1) & \text{if } \phi_A \geq 0, \phi_B < 0 \\ (1, 1) & \text{if } \phi_A < 0, \phi_B < 0 \end{cases} \quad \text{(A.7)}$$

$$\arg\max_{i',j'} f = \begin{cases} (1, 1) & \text{if } \phi_A \geq 0, \phi_B \geq 0 \\ (\sqrt{M}, 1) & \text{if } \phi_A < 0, \phi_B \geq 0 \\ (1, \sqrt{M}) & \text{if } \phi_A \geq 0, \phi_B < 0 \\ (\sqrt{M}, \sqrt{M}) & \text{if } \phi_A < 0, \phi_B < 0 \end{cases} \quad \text{(A.8)}$$

Substituting these minimum and maximum values as expressed in (A.5)–(A.8) into (A.3) and (A.4), we can obtain a constraint among ϕ_A, ϕ_B and M:

$$\begin{aligned} \frac{\sqrt{2}}{2}\big(\cos(\phi_A) &+ \cos(\phi_B) - \sin(|\phi_A|) - \sin(|\phi_B|)\big) \\ &= \cos\left(|\phi_A| + \frac{\pi}{4}\right) + \cos\left(|\phi_B| + \frac{\pi}{4}\right) \\ &> \frac{2\sqrt{M} - 3}{\sqrt{2}(\sqrt{M} - 1)}. \end{aligned} \quad \text{(A.9)}$$

Note that from (A.3)–(A.8), we have $\min_{i,i',j,j'} f = -\max_{i,i',j,j'} f$. Hence, the two inequalities in (A.3) merge into one inequality in (A.9).

ACKNOWLEDGMENT

This work is supported by the Fundamental Research Funds for the Central Universities under Grant No. N100404008.

REFERENCES

[1] S. Zhang, S. C. Liew, and P. P. Lam, "Hot topic: Physical-layer network coding," in *Proc. ACM MobiCom*, Sep. 2006, pp. 358–365.

[2] P. Popovski and H. Yomo, "The anti-packets can increase the achievable throughput of a wireless multi-hop network," in *Proc. IEEE ICC*, Jun. 2006, pp. 3885–3890.

[3] K. Lee and L. Hanzo, "Resource-efficient wireless relaying protocols," *IEEE Wireless Commun. Mag.*, vol. 17, no. 2, pp. 66–72, Apr. 2010.

[4] M. Noori and M. Ardakani, "On symbol mapping for binary physical-layer network coding with PSK modulation," *IEEE Trans. Wireless Commun.*, vol. 11, no. 1, pp. 21–26, Jan. 2012.

[5] H. J. Yang, Y. Choi, and J. Chun, "Modified high-order PAMs for binary coded physical-layer network coding," *IEEE Commun. Lett.*, vol. 14, no. 8, pp. 689 –691, Aug. 2010.

[6] M. P. Wilson, K. Narayanan, H. D. Pfister, and A. Sprintson, "Joint physical layer coding and network coding for bidirectional relaying," *IEEE Trans. Inf. Theory*, vol. 56, no. 11, pp. 5641–5654, Nov. 2010.

[7] W. Nam, S.-Y. Chung, and Y. H. Lee, "Capacity of the gaussian two-way relay channel to within 1/2 bit," *IEEE Trans. Inf. Theory*, vol. 56, no. 11, pp. 5488–5494, Nov. 2010.

[8] D. Wang, S. Fu, and K. Lu, "Channel coding design to support asynchronous physical layer network coding," in *Proc. IEEE GLOBECOM*, Mar. 2009, pp. 1–6.

[9] T. Koike-Akino, P. Popovski, and V. Tarokh, "Optimized constellations for two-way wireless relaying with physical network coding," *IEEE J. Sel. Areas Commun.*, vol. 27, no. 5, pp. 773–787, Jun. 2009.

[10] L. Lu, S. C. Liew, and S. Zhang, "Optimal decoding algorithm for asynchronous physical-layer network coding," in *Proc. IEEE ICC*, Jun. 2011, pp. 1–6.

[11] R. Mudumbai, G. Barriac, and U. Madhow, "On the feasibility of distributed beamforming in wireless networks," *IEEE Trans. Wireless Commun.*, vol. 6, no. 5, pp. 1754–1763, May 2007.

[12] Y. Yang and R. S. Blum, "Phase synchronization for coherent MIMO radar: Algorithms and their analysis," *IEEE Trans. Signal Process.*, vol. 59, no. 11, pp. 5538–5557, Nov. 2011.

[13] S. Sigg, R. M. E. Masri, and M. Beigl, "Feedback-based closed-loop carrier synchronization: A sharp asymptotic bound, an asymptotically optimal approach, simulations, and experiments," *IEEE Trans. Mobile Comput.*, vol. 10, no. 11, pp. 1605–1617, Nov. 2011.

[14] Y. Huang, Q. Song, S. Wang, and A. Jamalipour, "Phase-level synchronization for physical-layer network coding," to appear at IEEE GLOBECOM 2012.

[15] W. U. Bajwa, J. Haupt, A. M. Sayeed, and R. Nowak, "Compressed channel sensing: A new approach to estimating sparse multipath channels," *Proc. IEEE*, vol. 98, no. 6, pp. 1058–1076, Jun. 2010.

[16] J. G. Proakis, *Digital Communications*, 4th ed. Boston: McGraw-Hill, 2001.

[17] K. Yasami and A. Abedi, "Effect of channel estimation error on performance of physical layer network coding," in *Proc. IEEE CCNC*, Jan. 2011, pp. 973–974.

[18] K. Lu, S. Fu, Y. Qian, and H.-W. Chen, "SER performance analysis for physical layer network coding over AWGN channels," in *Proc. IEEE GLOBECOM*, Dec. 2009, pp. 1–6.

[19] M. Park, I. Choi, and I. Lee, "Exact BER analysis of physical layer network coding for two-way relay channels," in *Proc. IEEE VTC*, May 2011, pp. 1–5.

[20] M. Ju and I.-M. Kim, "Error performance analysis of BPSK modulation in physical-layer network-coded bidirectional relay networks," *IEEE Trans. Commun.*, vol. 58, no. 10, pp. 2770–2775, Oct. 2010.

[21] J. W. Craig, "A new, simple and exact result for calculating the probability of error for two-dimensional signal constellations," in *Proc. IEEE MILCOM*, Nov. 1991, pp. 571–575 vol.2.

[22] S. Wang, Q. Song, L. Guo, and A. Jamalipour, "Constellation mapping for physical-layer network coding with M-QAM modulation," to appear at IEEE GLOBECOM 2012.